JOURNAL OF AIRCRAFT
Vol. 48, No. 3, May–June 2011

Approach to Assess Bird Strike Resistance for a Wing Slat Structure

P. Xue,* N. Zhao,† J. Liu,‡ and Y. L. Li*
Northwestern Polytechnical University, 710072 Xi'an, People's Republic of China

DOI: 10.2514/1.C031240

This study presents an approach to assess the bird strike resistance of an aircraft wing slat structure. The slat is made of 2024 aluminum that can be described by an elastic–plastic strain-rate-dependent model with damage. The bird is modeled using smooth particle hydrodynamics. The constants included in the smooth particle hydrodynamics model are determined by experiments. The performance of the wing slat structure after a bird strike is simulated and analyzed. Based on the partition of dissipation energy, it can be seen that when the skin of the leading edge is not penetrated after a bird strike, the large plastic deformation of upper skin contributes most to the impact energy dissipation. The slat spar is the next in the hierarchy of damage, and then the ribs near the striking location. The rivets connecting the skin to the ribs are found to have a significant effect on the performance of the structure. Rivet failure that has occurred in the proper region is helpful to avoid bird penetration. Through deep investigation of the behavior of slat components in withstanding a bird strike, the capacity of bird strike resistance for a wing slat can be assessed, and the structural design can be guided.

I. Introduction

BIRD-STRIKING has been a growing threat to civil and military aircraft safety. The U.S. Department of Transportation, the Ministry of Agriculture, and the Federal Aviation Administration (FAA) issued statistical data indicating that a total of 89,727 bird strike events happened on civil aircraft from 1990 to 2008 in the United States, resulting in huge economic and life losses [1]. The economic cost to the worldwide aviation industry was estimated to be over 1 billion U.S. dollars per year [2]. In recent years, bird strike events have attracted more and more attention.

During aircraft flight, the windward parts of an aircraft are vulnerable to bird strike, such as engines, radar cover, windshield, wing leading edge, tail, and so on. Among them, the engine is the most commonly damaged component, and the next one is the wing [3]. The bird strike resistance capability of the structure must be considered in designing, especially for civil aircraft.

The wing is usually equipped with a movable leading edge or slats. Figure 1 shows two positions at which the slat is fully retracted and fully extended [4]. For bird strike resistance of a wing slat, birds should not penetrate the skin of the leading edge and, even penetrated, the structural elements behind the skin should not be damaged in the worst case. Therefore, the slats have to meet not only the aerodynamic design, strength, and stiffness requirements but also the requirements of bird strike resistance. Simply increasing the structure strength can improve its capability of bird strike resistance, but this will increase the weight of structure, thus affecting aircraft performance and increasing costs. For these reasons, aircraft engineers prefer to use new materials and design new structures to meet the requirements of bird strike resistance.

Some studies have been done on the bird strike resistance of wing leading edges. McCarthy et al. [5] presented a bird model in a bird strike event. Zhang and Li [6] and Wan et al. [7] investigated the performance of airplane leading edges after bird striking. Rueda et al. [8] assessed the bird strike resistance for the EF-2000 under different impact scenarios. The investigations so far have still not gone far enough.

This study will analyze the performance of a wing slat under a bird strike; in addition, it will assess the capability of bird strike resistance for a given wing slat using a commercialized finite element dynamic software, PAM-CRASH. The roles of the constitutive components in absorbing the bird impact energy will be analyzed. The whole paper consists of four sections. In the following sections, descriptions of the materials and structure will be given first, followed by the results and discussions. Finally, some conclusions will be drawn.

II. Material and Structure Models

A. Wing Slat and Bird

A typical segment of the studied wing slat is shown in Fig. 2. The sweepback of the leading edge is θ. The slat mainly consists of the upper and lower skins, a spar, and a series of ribs. The average thickness of the upper and lower skins is 1.6 mm.

It is assumed that the bird strikes the slat at a speed of 150 m/s. The bird geometry is modeled as a circular cylinder with hemispherical end caps, with an aspect ratio of 2:1, as shown in Fig. 3. The density of the bird material is 950 kg/m^3 [9]. The diameter of the hemisphere ends is determined as 115 mm. From experimental observations and accident reports, it is known that birds behave in a fluidlike manner when striking at high speed, undergoing extreme distortion, and even breaking into debris.

The smooth particle hydrodynamics (SPH) model has no grid or strong antidistortion characteristics, thus overcoming the regular finite element mesh distortion problem. It has been found that modeling birds with SPH particles is the most popular method currently used in investigating bird strike phenomena [10–12]. The bird material for the SPH model can be described by the material 28 in PAM-CRASH, and the equation of state is given as

$$P = P_0 + B\left[\left(\frac{\rho}{\rho_0}\right)^{\gamma} - 1\right] \tag{1}$$

where P_o is a referrence pressure. The current density is ρ, and ρ_0 is the initial density. Constants B and γ are to be determined by experiments. Comparing with other bird models, this one only includes two parameters to be determined. In addition, ignored shear strength in this model can avoid the instability in the numerical simulation.

Received 16 September 2010; revision received 17 November 2010; accepted for publication 18 November 2010.

*Professor, School of Aeronautics, 127 Youyi Xilu. Member AIAA.
†Master Student, School of Aeronautics, 127 Youyi Xilu.
‡Postdoctoral Student, School of Aeronautics, 127 Youyi Xilu.

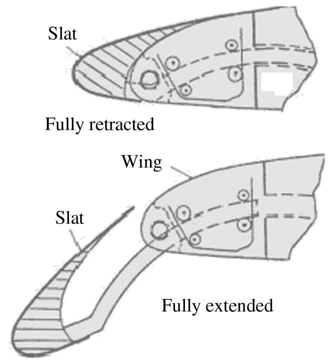

Fig. 1 Two positions where slat is fully retracted and fully extended.

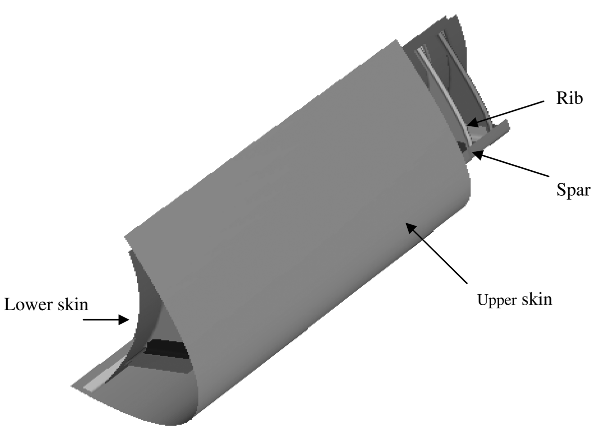

Fig. 2 Segment of a wing slat.

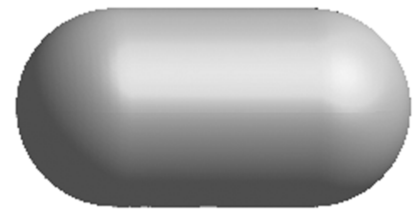

Fig. 3 Geometry of the bird model.

B. Determination of Constants in the Bird Model

Two constants in the bird model cannot be measured directly. In this study, an experimental setup was designed to determine the two parameters. Figures 4a and 4b show the experimental apparatus and the details for a bird strike test. A plate was clamped by bolts to a frame made of 45 carbon steel, then it was installed through force sensors to a fixture. A bird was shot by an air gun system at a velocity normal to the plate. The displacements at specified locations of D_1 and D_2 on the target, as shown in Fig. 4c, were measured by a laser measuring device. The optimization software iSIGHT, which incorporates a genetic algorithm and a sequence quadratic program algorithm, was applied. The optimization objective function was defined as

$$F = \left\{\frac{\mathrm{MAX}D1_C - \mathrm{MAX}D1_T}{\max[\mathrm{MAX}D1_C, \mathrm{MAX}D1_T]}\right\}^2 + \left\{\frac{\mathrm{MAX}D2_C - \mathrm{MAX}D2_T}{\max[\mathrm{MAX}D2_C, \mathrm{MAX}D2_T]}\right\}^2 \tag{2}$$

where $\mathrm{MAX}Di_C$ and $\mathrm{MAX}Di_T$ indicate the calculated and tested maximum displacements at points D_i on the plate ($i = 1$ or 2), respectively. By matching the optimized results with the tested results, the constants in the equation of state of the bird model can be determined as $B = 2.8$ GPa and $\gamma = 7.99$. It is also known that the constant γ has little effect on the displacement, while the constant B only affects the displacement closer to the impact point [13].

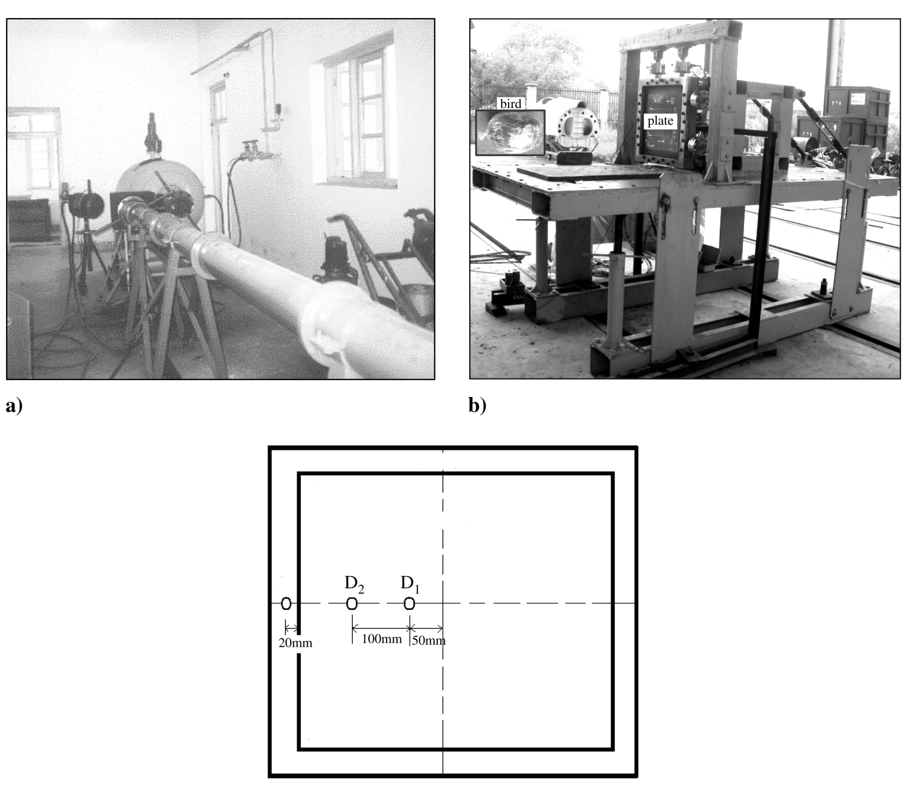

Fig. 4 Experimental apparatus and details for bird strike tests: a) air gun system, b) experimental setup, and c) two specified locations in measuring displacements.

Table 1 Constants in the Johnson–Cook model

Constant	Value
A	325
B	555
C	−0.001
n	0.28
m	2.2
T_{melt}, K	775

C. Metallic Constitutive Model

The slats are mostly made of 2024 aluminum alloy. This material can be described by the Johnson–Cook model as

$$\sigma = [A + B\varepsilon^n]\left[1 + C\,\ell n\,\frac{\dot{\varepsilon}}{\dot{\varepsilon}_0}\right]\left[1 - \left(\frac{T - T_r}{T_{\mathrm{melt}} - T_r}\right)^m\right] \tag{3}$$

The experimental results reported in [14] can be used to obtain the parameters included in this model. They are given in Table 1. A damage model with a maximum effective strain is introduced. The elements are eventually eliminated when a certain level of effective plastic strain ε_f is reached at least at one of the integration points through the thickness. In this study, $\varepsilon_f = 0.19$. The rivet is made of aluminum alloy, and its diameter is 4.75 mm.

D. Numerical Model

The wing slat is discretized by four node shell elements, S4R, with reduced integration and hourglass control. The total number of elements is 82,076. Three integration points along the thickness are set. The number of SPH particles is 5440.

The connections are located at the actual rivet positions. The mechanically fastened joints are represented by PAM-CRASH PLINK elements. The number of PLINK elements is 686. Rivet rupture is taken into account by the failure criterion as

$$\left(\frac{N}{T_{\max}}\right)^m + \left(\frac{T}{S_{\max}}\right)^n = 1 \tag{4}$$

where N and T are the tensile force and shear force, respectively. The maximum tensile force $T_{\max}$ and shear force $S_{\max}$, along with the exponents, are used to consider their interaction effects. Referring to [5], $T_{\max}$ and $S_{\max}$ are taken as 5100 and 3200, respectively, and $m = 1.5$ and $n = 2.1$. The whole numerical model, including the bird and the wing slat, is shown in Fig. 5.

III. Results and Discussions

Figure 6 shows the deformed slat structure at different moments after the bird strike, at a speed of 150 m/s. It can be seen that the upper skin remains integrated and is not penetrated after the bird strike, although (finally) very large deformation appears on the upper skin. During the bird strike, the kinetic energy of the bird is absorbed mainly by the large plastic deformation of the structure. Figure 7 shows the kinetic energy of the bird varies with time. It can be seen that, from the beginning to 3 ms, the kinetic energy of the bird decays rapidly. Afterward, due to the sweepback angle of the leading edge and the rivet restraint, the bird mainly slides along the spanwise direction from the impact point to the wing tip at an almost constant speed, leaving an oblong dent on the skin. In this stage, the kinetic energy of the bird remains almost unchanged.

Table 2 gives the partition of the total energy in dissipating the bird kinetic energy. As can be seen, the upper skin absorbs the impact energy up to 9232.75 J, about 67% of the total energy. It contributes

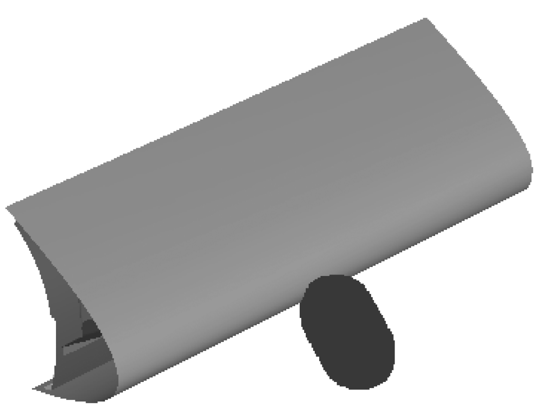

Fig. 5 Numerical model.

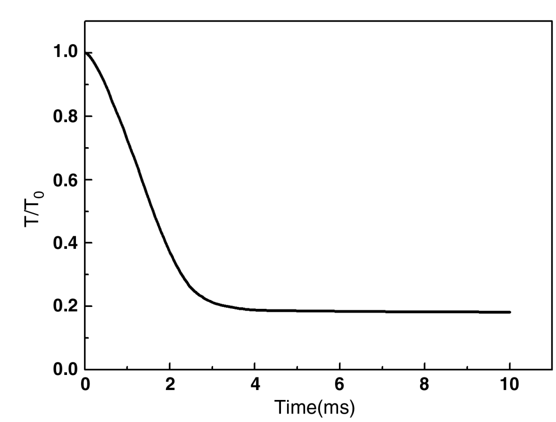

Fig. 7 Kinetic energy of the bird varying with time.

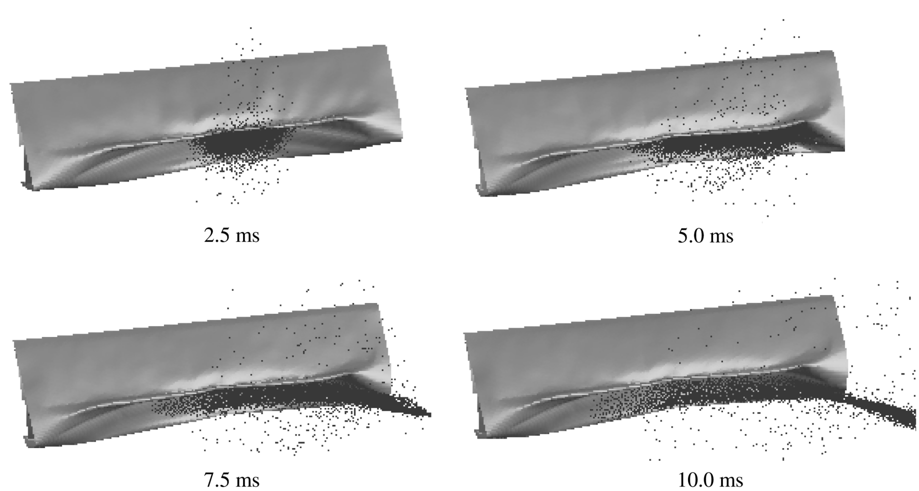

Fig. 6 Deformed slat structure at different moments after a bird strike.

Table 2 Partition of the total absorbed energy after the bird strike

	Bird	Upper skin	Spar	Rib	Stringer	Lower skin	Other
Absorbed energy, J	3013.85	9232.75	495.04	483.09	117.95	179.99	212.11
Percentage, %	21.94	67.22	3.60	3.52	0.86	1.31	1.54

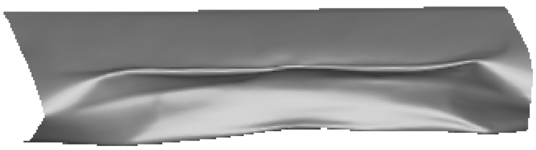

Fig. 8 Deformed upper skin after bird strike.

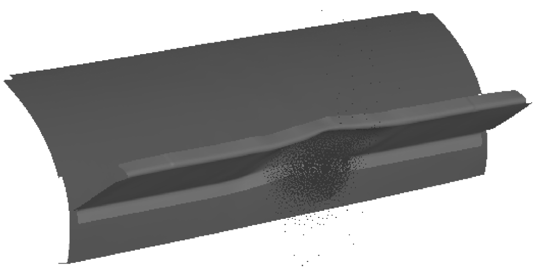

Fig. 9 Deformed spar after bird strike.

most in dissipating the bird kinetic energy. The final configuration of the deformed upper skin is shown in Fig. 8. In addition, the birds can dissipate up to 3013.85 J, about 22% the total energy. The slat spar is the next in the hierarchy of damage shown in Fig. 9, then the ribs near the striking location. Correspondingly, both also absorb some impact energy. The ribs play as stiffening components and prevent the structure from more severe damage. By comparing with Fig. 8, it is shown that the deformed extent of the skin is much more serious than that of the spar. The spar only experiences local damage in the impact area.

It is also noticed that the rivets connecting the skin to the ribs have a profound effect on the performance of the structure. Rivet failure that occurs in the proper region is helpful to avoid bird penetration.

IV. Conclusions

This study presents an approach to assess the bird strike resistance of a wing slat structure. Based on finite element simulation, a comprehensive understanding of the slat behavior after bird striking is obtained. The roles of constitutive components in dissipating the bird impact energy are identified. Some conclusions can be drawn:

1) The SPH method is proved to be effective in describing the phenomena of bird breakup into debris in a bird striking event. It can avoid the instability problem in simulation.

2) Plastic deformation of the slat upper skin contributes most in dissipating the bird kinetic energy. The bird itself also dissipates about 22% of the total energy. The spar is the next in the hierarchy of damage, then the ribs near the striking location. Both absorbed some impact energy.

3) Rivet failure that occurs in the proper region is helpful to avoid bird penetration.

Acknowledgments

This work is supported by the Civil Aviation Special Fund from the Commission of Science, Technology, and Industry of China. The authors also gratefully acknowledge financial support from the National Science Foundation of China, under grants 10872168 and 11072202.

References

[1] Dolbeer, R. A., Wright, S. E., Weller, J., and Begier, M. J., "Wildlife Strike to Civil Aircraft in the United States 1990–2008," Federal Aviation Administration, Office of Airport Safety and Standards, Washington, D.C., 2009.

[2] Safety Regulation Group, "Completeness and Accuracy of Bird-Strike Reporting in the UK," Civil Aviation Authority Paper 2006/05, London, 2006.

[3] Cleary, E. C., Dolbeer, R. A., and Wright, S. E., "Wildlife Strikes to Civil Aircraft in the United States 1990–2002," Federal Aviation Administration, Office of Airport Safety and Standards, Serial Report 9, Washington, D.C., 2003.

[4] Niu, M. C. Y., *Airframe Structural Design*, Adaso Adastra Engineering Center, Northridge, CA, 2006.

[5] McCarthy, M. A., Xiao, J. R., McCarthy, C. T., Kamoulakos, A., Ramos, J., Gallard, J. P., and Melito, V., "Modeling of Bird Strike on an Aircraft Wing Leading Edge Made from Fibre Metal Laminates: Part 2: Modelling of Impact with SPH Bird Model," *Applied Composite Materials*, Vol. 11, No. 5, 2004, pp. 317–340. doi:10.1023/B:ACMA.0000037134.93410.c0

[6] Zhang, Y. K., and Li, Y. L., "Analysis on Bird-Strike Resistance for Aircraft Beam Structures," *Journal of Mechanical Science and Technology*, Vol. 26, No. 12, 2007, pp. 1595–1599.

[7] Wan, X. P., Gong, L., Zhao, M. Y., and Hou, C., "Investigation on Bird-Strike Resistance for an Leading Edge Based on ANSYS/LS-DYNA Simulation," *Transaction of Northwestern Polytechnical University*, Vol. 25, No. 2, 2007, pp. 285–289.

[8] Rueda, F., Beltrán, F., Maderuelo, C., and Climent, H., "Birdstrike Analysis of the Wing Slats of EF-2000," *Structures and Materials*, Vol. 11, 2002, pp. 189–198.

[9] "Civil Aviation Administration Rules," Civil Aviation Administration of China, Beijing, PRC, 1995.

[10] Ubels, L. C., Johnson, A. F., Gallard, J. P., and Sunaric, M., "Design and Testing of a Composite Bird-Strike Resistant Leading Edge," National Aerospace Laboratory/NLR TP 2003-054, The Netherlands, 2003.

[11] Lin, I-Chien, "A Study of Soft Bird Model Impacting on Flat Plate and Aircraft Pylon," M.S. Thesis, National Cheng Kung Univ., Taiwan, ROC, 2006.

[12] Anghileri, M., Castelletti, L. L., Mazza, V., "Birdstrike: Approaches to the Analysis of Impacts with Penetration," *WIT Transactions on Engineering Sciences*, Vol. 49, 2005, pp. 63–74.

[13] Liu, J., and Li, Y. L., "The Optimization Inversion on Bird Constitutive Model Parameters and the Simulation on Bird Striking," *Acta Aeronautica et Astronautica Sinica*, accepted for publication.

[14] Li, N., Li, Y. L., and Guo, W. G., "Comparison Studies of Dynamic and Temperature Related Properties for Three Kinds of Al Alloys," *Acta Aeronautica et Astronautica Sinica*, Vol. 29, No. 4, 2008, pp. 903–908.